Interaction of Fluorescently-labeled Contractile Proteins with the Cytoskeleton in Cell Models

JOSEPH W. SANGER, BALRAJ MITTAL, and JEAN M. SANGER
Department of Anatomy and the Pennsylvania Muscle Institute, University of Pennsylvania School of Medicine, Philadelphia, Pennsylvania 19104

ABSTRACT To determine if a living cell is necessary for the incorporation of actin, alpha-actinin, and tropomyosin into the cytoskeleton, we have exposed cell models to fluorescently labeled contractile proteins. In this in vitro system, lissamine rhodamine-labeled actin bound to attachment plaques, ruffles, cleavage furrows and stress fibers, and the binding could not be blocked by prior exposure to unlabeled actin. Fluorescently labeled alpha-actinin also bound to ruffles, attachment plaques, cleavage furrows, and stress fibers. The periodicity of fluorescent alpha-actinin along stress fibers was wider in gerbil fibroma cells than it was in PtK_2 cells. The fluorescent alpha-actinin binding in cell models could not be blocked by the prior addition of unlabeled alpha-actinin suggesting that alpha-actinin was binding to itself. While there was only slight binding of fluorescent tropomyosin to the cytoskeleton of interphase cells, there was stronger binding in furrow regions of models of dividing cells. The binding of fluorescently labeled tropomyosin could be blocked by prior exposure of the cell models to unlabeled tropomyosin. If unlabeled actin was permitted to polymerize in the stress fibers in cell models, fluorescently labeled tropomyosin stained the fibers. In contrast to the labeled contractile proteins, fluorescently labeled ovalbumin and BSA did not stain any elements of the cytoskeleton. Our results are discussed in terms of the structure and assembly of stress fibers and cleavage furrows.

Actin and proteins that associate with actin such as tropomyosin, myosin, and alpha-actinin are distributed in nonmuscle cells in patterns that are characteristic for each protein (11, 20, 21, 22, 29, 38, 49). In a variety of different cell types, actin has been localized by the use of fluorescent staining agents in stress fibers, ruffles, attachment plaques, and cell junctions (22, 29, 31, 38). Some studies also show it to be concentrated in both cleavage furrows and mitotic spindles (6, 29, 30, 32, 36, 37), whereas others find actin in either the spindle (16, 48, 49) or the furrow (1–3, 14), but not in both. In stress fibers, actin usually appears to be distributed continuously along the length of the fibers (22, 29, 30), although in a few cases, its distribution is discontinuous (15, 31). Tropomyosin is localized in a striated pattern along stress fibers and appears to be absent from areas where alpha-actinin is present, i.e., stress fiber densities, ruffles, cell junctions, attachment plaques, and foci of polygonal networks (20, 38). Like tropomyosin, alpha-actinin is found in a striated pattern along stress fibers (21, 38). Colocalization studies indicate that the two proteins are in adjacent bands (15, 52).

In experiments where fluorescently labeled actin, tropomyosin, or alpha-actinin have been injected into living cells, they become localized in precisely the areas where previous studies with antibodies or actin-binding agents have shown them to be concentrated (7, 18, 35, 37, 40, 45, 50). Observations of cells injected with labeled actin or alpha-actinin show that the injected proteins behave in the same way as endogenous actin and alpha-actinin when living cells are followed in time-lapse or experimentally manipulated (7, 17, 35, 40, 47, 50). Although injected tropomyosin appears to be localized along the whole length of stress fibers rather than in a striated pattern, it is excluded from ruffles and attachment plaques (50). If cells that have been injected with fluorescent tropomyosin are treated with phalloidin or cytochalasin-B, the fluorescent tropomyosin becomes localized in aggregates in the same way as the endogenous tropomyosin (50). These experiments all suggest that injected fluorescent proteins are selectively incorporated by living cells into structures and domains where their endogenous counterparts are localized and that once incorporated they respond in the same way as the cells' own proteins. In this study, we have exposed cell models to fluorescently labeled actin, alpha-actinin, and tro-

THE JOURNAL OF CELL BIOLOGY · VOLUME 99 SEPTEMBER 1984 918-928

pomyosin to see if a living cell is necessary for incorporation of these proteins into the cytoskeleton and if self-assembly or protein-protein interactions play a role in the process of incorporation.

MATERIALS AND METHODS

Cell Cultures: PtK_2 cells, an epithelial line, and gerbil fibroma cells (American Tissue Type Collection, Rockville, MD) were grown on glass coverslips in culture dishes as described previously (30, 38). Chick fibroblasts and epithelial cells were obtained from primary and secondary cultures of embryonic cardiac muscle and grown on glass coverslips (32). The medium used was Eagle's minimal medium supplemented with 10% fetal calf serum, 1% antibiotic (10,000 U penicillin, 10,000 μg streptomycin, 25 μg Fungizone), and 1.5% glutamine (all obtained from GIBCO Laboratories, Grand Island, NY).

Preparation of Cell Models: Cell models were made in three different ways. (*a*) The medium in the culture dishes was removed and replaced with a cold solution (4°C) of 25% glycerol in standard salt solution (0.1 M KCl, 0.01 M phosphate buffer, 0.001 M $MgCl_2$, pH 7.0). The cells were kept in this cold solution for 2 h in the refrigerator (4°C) and then washed with cold standard salt and exposed to labeled proteins. (*b*) The medium in the dishes was removed and the cells placed in 0.02% Nonidet P-40 in standard salt solution for 1–5 min at 22°C, then washed with cold standard salt before being exposed to labeled proteins. (*c*) Finally, some cells on coverslips were exposed to cold acetone (−20°C) for 10 s to 5 min, and washed with cold standard salt solution (4°C) before staining.

Preparation of Fluorescently Labeled Proteins: F-actin was prepared from acetone powder of rabbit skeletal muscle by standard procedures (25). Tropomyosin and alpha-actinin were purified from fresh or frozen chicken gizzards (8, 41, 45). Crystalline BSA and ovalbumin were purchased from Sigma Chemical Co. (St. Louis, MO). Lissamine rhodamine sulfonyl chloride (LR)[1] was obtained from Molecular Probes (Junction City, OR). The proteins were labeled with the fluorescent dye essentially by the method of Brandtzaeg (5).

F-actin was dialyzed overnight against 0.1 M KCl and 0.05 M sodium bicarbonate (pH 9.0) and lissamine rhodamine sulfonyl chloride was added in powder form (25 μg/mg protein; protein concentration 4–6 mg/ml). The labeling was carried out for 1–2 h at 4°C, and the reaction was terminated by adding 1 M NH_4 Cl solution to a final concentration of 50 mM. The labeled protein was dialyzed for 2 d against several changes of depolymerizing buffer (0.2 mM ATP, 2 mM Tris, 0.2 mM $CaCl_2$, 0.5 mM beta-merceptoethanol, and 0.005% NaN_3, pH 8.0) (22), and then centrifuged for 3 h at 80,000 *g* to remove aggregates. The monomer actin-LR was cycled through one more polymerization-depolymerization cycle before the monomer actin-LR was adsorbed to a DEAE cellulose column (DE-52, Whatman, Inc., Clifton, NJ) equilibrated with depolymerization buffer. Actin-LR was eluted with 0–0.5 M gradient of KCl in the depolymerization buffer. The labeled protein fractions that eluted between 0.3–0.5 M KCl were pooled, polymerized, and depolymerized as described above. The dye/protein molar ratio was between 1 and 2 (5). Actin-LR was stored either as F-actin-LR at 0°C and converted to monomer form before use or stored as monomer in depolymerizing buffer in liquid nitrogen up to several months.

Before labeling, alpha-actinin was dialyzed against 1 mM potassium bicarbonate. 1 M sodium carbonate was added to the protein solution to give a final concentraiton of 0.2 M sodium carbonate, pH 9.0. The dye was mixed with the protein at 50 μg/mg protein for 2 h at 4°C. After spinning out the dye aggregates, unbound dye was removed with a Sephadex G-25 column (Pharmacia, Piscataway, NJ) equibrated with 20 mM Tris-acetate, 20 mM NaCl, 0.1 mM EDTA, 1 mM beta-merceptoethanol, pH 7.6, and the labeled protein was further subjected to DEAE cellulose chromatography. The protein used for our experiments eluted between 0.27 and 0.37 M KCl and had a dye/protein molar ratio between 1 and 2. It was stored in a 50% glycerol-standard salt solution at 0°C.

Tropomyosin was first dialyzed overnight with 0.2 M KCl, 0.01 M sodium phosphate, pH 7.4. Before the protein was labeled, Na_2CO_3 was added to make the solution 0.2 M Na_2CO_3 and pH 9.0. Labeling was carried out for 1 h at 4°C with 25 μg dye/mg protein. Unbound dye was removed with Sephadex G-25 (equilibrated with 10 mM Tris-HCl buffer, pH 7.6) and the tropomyosin-LR solution then adsorbed to DEAE cellulose. The protein eluting between 0.15–0.25 M NaCl was used in the experiment. The tropomyosin-LR was concentrated by isoelectric precipitation at pH 4.3–4.6 (41). The dye/protein molar ratio was between 1 and 2.

The conditions for labeling of BSA and ovalbumin were similar to those for alpha-actinin. However these proteins were not placed on a DEAE-cellulose column. The dye/protein molar ratio was between 2 and 3.

[1] *Abbreviation used in this paper:* LR, lissamine rhodamine.

Gel Electrophoresis and Protein Assays: A 7.5% acrylamide gel was used in Laemmli's buffer system (19). Protein samples were boiled in SDS buffer (1% SDS, 1% beta-mercaptoethanol, 10 mM Tris-HCl, 10% glycerol, pH 6.8) and 10–20 μg protein were loaded into each lane. After electrophoresis, gels were fixed in methanol-acetic acid solution (40% methanol, 10% acetic acid) and the bands visualized either unstained under ultraviolet light or stained with Coomassie Blue (Fig. 1).

The concentrations of purified unlabeled contractile proteins were determined spectrophotometrically using the following values for $A^{1\%}_{280}$: G-actin, 11.0 (4), alpha-actinin, 9.7 (43), tropomyosin, 3.0 (51). The concentrations of the LR-labeled proteins and dye/protein ratios were determined spectrophotometrically using the formulae derived by Brandtzaeg (5).

The specificity of the various labeled proteins was tested by using myofibrils as assay systems (33). Alpha-actinin-LR stained Z-bands (Fig. 2, *a* and *b*). Myofibrils stained with monomer actin-LR (in the absence of ATP) yielded doublets of staining in the H-zone (Fig. 2, *c* and *d*). Tropomyosin-LR did not stain control myofibrils unless unlabeled actin was added first. In this case (Fig.

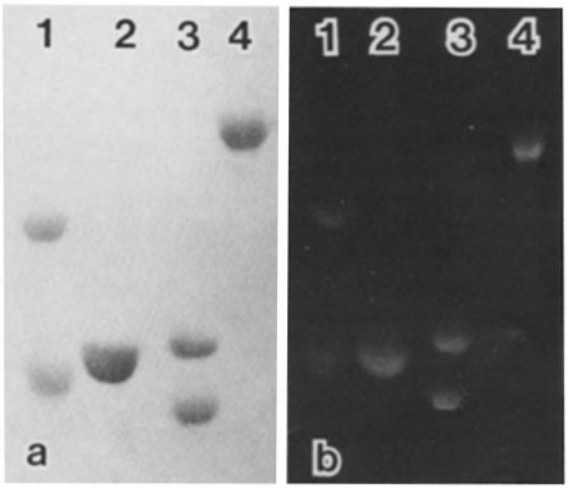

FIGURE 1 (*a*) Coomassie Blue-stained gel of purified fluorescently labeled proteins. Lane *1* contains BSA-LR (*top;* 66 kdaltons) and ovalbumin-LR (*bottom;* 43 kdaltons). Lane *2* contains actin-LR. Lane *3* contains gizzard tropomyosin-LR, alpha and beta chains. Lane *4* contains alpha-actinin-LR. (*b*) The same fluorescently-labeled purified proteins as in Fig. 1 *a* photographed with ultraviolet light. Lanes *1–4* in Fig. 1 *b* correspond to lanes *1–4* in Fig. 1 *a*.

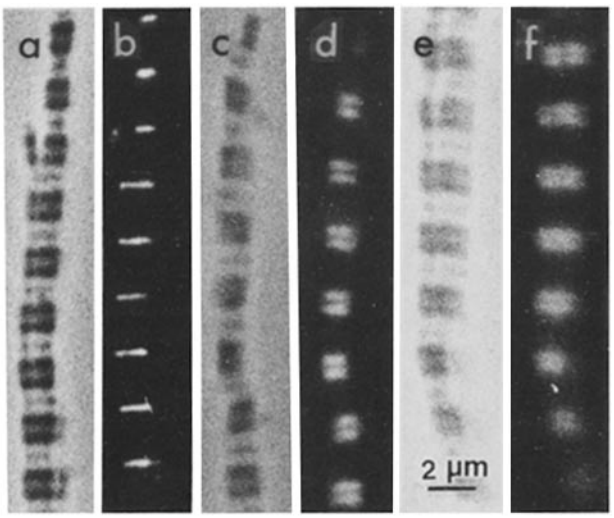

FIGURE 2 Phase and fluorescent micrograph pairs of myofibrils exposed to (*a* and *b*) alpha-actin-LR, (*c* and *d*) actin-LR, and (*e* and *f*) unlabeled actin followed by tropomyosin-LR. Alpha-actinin-LR binding (*b*) is confined to the Z-bands. Actin-LR binding (*d*) is confined to a doublet in the H-zone. Tropomyosin-LR which does not bind to control myofibrils (not shown), binds in a doublet in the H-zone (*f*) to myofibrils pretreated with unlabeled actin. No tropomyosin-LR binds in the I-band. × 3,000.

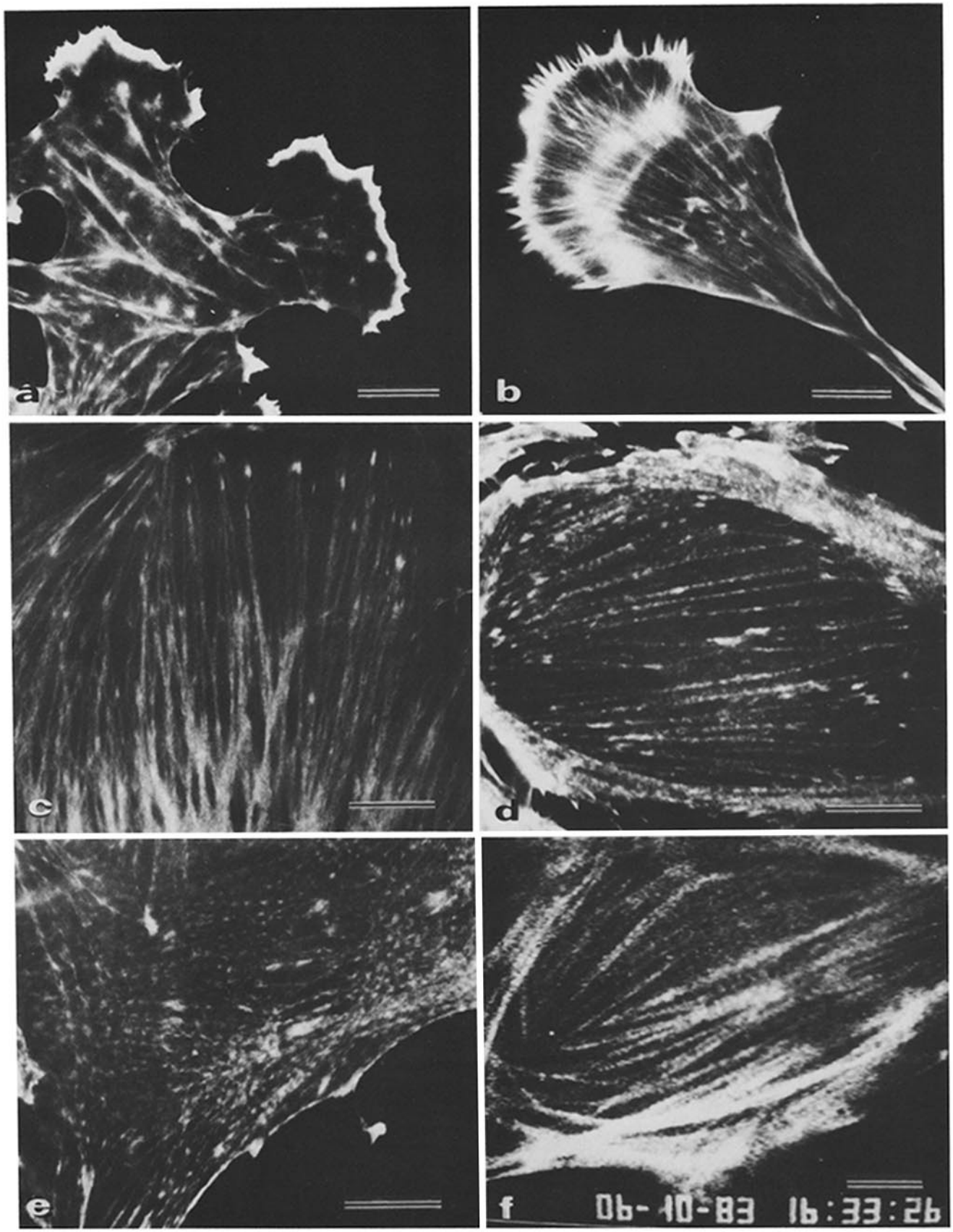

FIGURE 3 Actin-LR binding. (a) Glycerinated chick cardiac epithelial cell with actin-LR in ruffles and stress fibers; (*b*) glycerinated chick cardiac fibroblasts with actin-LR in filopodia, ruffle, stress fibers, and arc near the dorsal surface of the cell; (c) detergent-treated PtK_2 cells with actin-LR bound to stress fibers and attachment plaques; (*d*) glycerinated PtK_2 cell in which actin-LR bound in a periodic pattern to stress fibers; (e) glycerinated gerbil fibroma cell with periodic pattern of actin-LR binding; (*f*) videomicrograph of a living PtK_2 cell that has been microinjected 2 h previously with actin-LR. Bars, 10 μm. × 1,500 (*a–c*); × 1,700 (*d* and e); × 1,400 (*f*).

2, *e* and *f*), we obtained doublet patterns identical to actin-LR patterns (Fig. 2, *c* and *d*). When the proteins were over-labeled or too old, a lot of nonspecific binding occurred. This was particularly true of actin-LR which could reversibly polymerize when labeled with an excess of fluorochromes, but which produced continuous myofibrillar staining rather than doublet staining if over-labeled. When we used labeled proteins that stained myofibrils as in Fig. 2, we rarely observed nuclear staining in our cell models and microinjected living cells. Over-labeled proteins often stained mitochondria, nuclei, and nucleoli of cell models.

Addition of Labeled Proteins to Cell Models: After F-actin-LR was converted to monomer actin-LR, it was necessary to remove any unbound ATP so that any contraction of the cell model would be inhibited and binding of actin to myosin would not be inhibited. To do this, monomer actin-LR was treated with Dowex-1 (Sigma Chemical Co., St. Louis, MO) for 10 min, and the Dowex beads then spun down leaving monomer actin-LR. 100 μl of the actin (0.5–1 mg/ml) was added to cell models that were incubated with the protein for 30–60 min at 4°C, washed in several changes of standard salt, fixed with 3% paraformaldehyde (34), and mounted on a slide in 25–50% glycerol in standard salt.

100 μl tropomyosin-LR, alpha-actinin-LR, BSA-LR, or ovalbumin-LR in a standard salt solution were each added to cell models at a concentration of 0.5–1 mg/ml for 1 h at 4°C. The cell models were washed, fixed, and mounted as described for actin-LR. For some experiments, unlabeled monomer actin (1–2 mg/ml), tropomyosin (1–3 mg/ml), or alpha-actinin (2–5 mg/ml) was added to the cell models for an hour at 4°C, and the cell models then rinsed several times before labeled protein was added. Processing was carried out as described for addition of a single labeled protein.

Microinjection of Labeled Proteins into Living Cells: Cells were microinjected with labeled proteins that had passed the myofibril assay tests described above. The cells were placed on glass coverslips and microinjected using techniques previously described (26). Fresh medium was used to wash the cells, and after various time periods of incubation at 37°C, the glass slides were mounted with a vasoline seal on a glass slide. A heat curtain at 37°C was used during microscopic study of the injected cells.

Microscopy: The stained cells on coverslips were rinsed with a 25% glycerol solution in standard salt solution (see above) and mounted in this solution on a glass slide. The coverslip was then sealed with clear nail polish. These preparations as well as mounted living microinjected cells were examined with an Olympus Vanox Photomicroscope equipped for epifluorescence. The objectives used were Zeiss Planapochromats, ×63 and ×100. Images were recorded using Kodax Tri-X film developed with Acufine (Acufine, Inc., Chicago, IL) for an ASA rating of 1,000. Microinjected cells were viewed with a SIT camera and the images photographed off the TV monitor as described previously (26).

RESULTS

Addition of Fluorescent Actin to Cell Models

When monomer actin coupled to lissamine rhodamine (LR) was added to permeabilized cells in the absence of ATP in a standard salt solution that permits actin polymerization, ruffles, filopodia, stress fibers, and attachment plaques were labeled (Fig. 3, *a–e*). In most cases the stress fiber labeling in cells was continuous, the same pattern produced by actin antibodies (22) and other actin staining agents (3, 29, 30). In some PtK_2 and gerbil cell models, the fluorescence was discontinuous along the fiber (Fig. 3, *d* and *e*). The spacing between the fluorescent bands was longer in the fibroma cell (Fig. 3*e*) than in the epithelial PtK_2 (Fig. 3*d*). This periodic actin staining of the stress fibers is present in 0–5% of cells stained and is unaffected by the time of exposure of the cell models to labeled actin. Exposure of the models to actin-LR for as little as 5 min resulted in the same low percentage of cells with striated stress fibers. When actin-LR was present in a striated pattern in stress fibers, all stress fibers in the cell were similarly banded. When the actin-LR was microinjected into living PtK_2 cells, the fluorescence along some stress fibers was continuous and along others it was banded (Fig. 3*f*). Several cells were found that had been permeabilized at telophase in the mitotic cycle (Fig. 4). In these cells, actin-LR was concentrated between the separated chromsomes in the cleavage furrow area (Fig. 4).

Actin-LR was also added to cell models in the presence of 2 mM ATP (Fig. 5*a*) or 2 mM sodium pyrophosphate (data not shown). In both cases, the actin-LR patterns were the same as those obtained in the absence of ATP (Fig. 3, *a–c*). We made an attempt to block the actin-LR binding in cell models by first adding unlabeled monomer actin to cell models for 30–60 min, washing out the unbound actin, and adding monomer actin-LR for 30 min. This procedure did not block the addition of fluorescent actin to the cell although

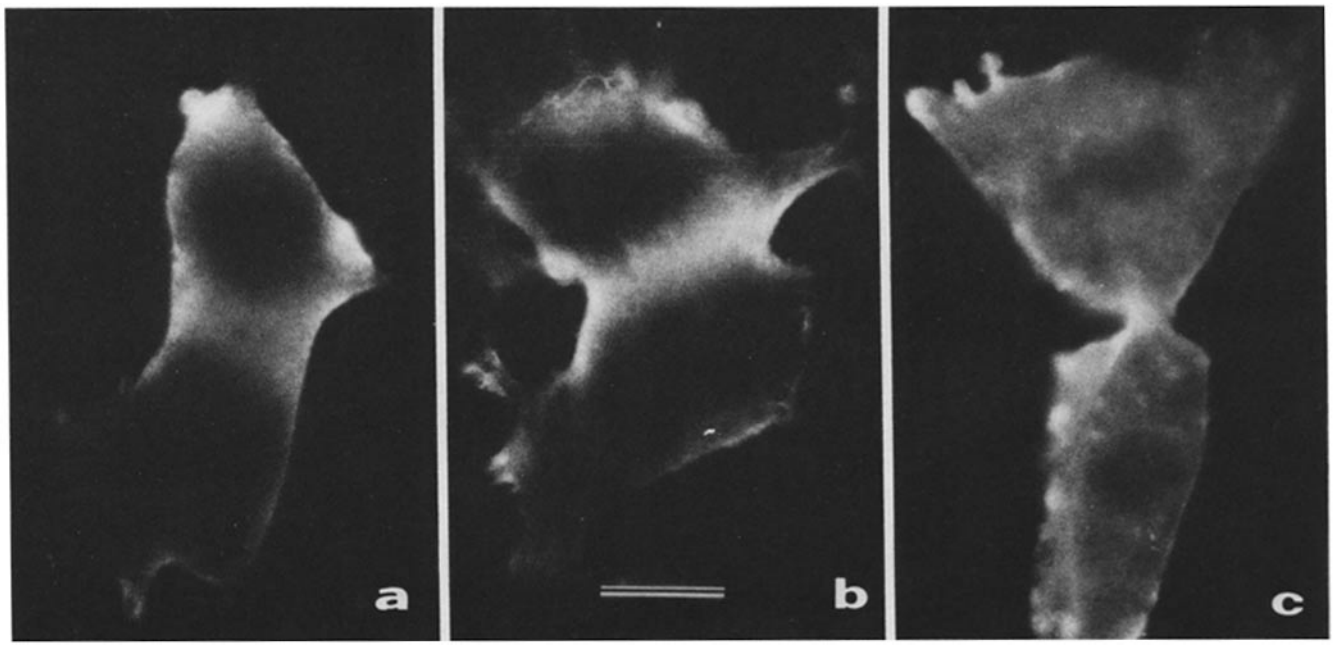

FIGURE 4 Glycerinated and detergent models of dividing PtK_2 cells exposed to actin-LR. (a) Glycerinated cell in early cleavage with broad belt of actin-LR in furrow region; (*b*) detergent-treated cell in mid-cleavage; (c) near the end of cytokinesis, actin-LR bound in the furrow and diffusely throughout the cytoplasm of this glycerinated cell. Bar, 10 μm. × 1,700.

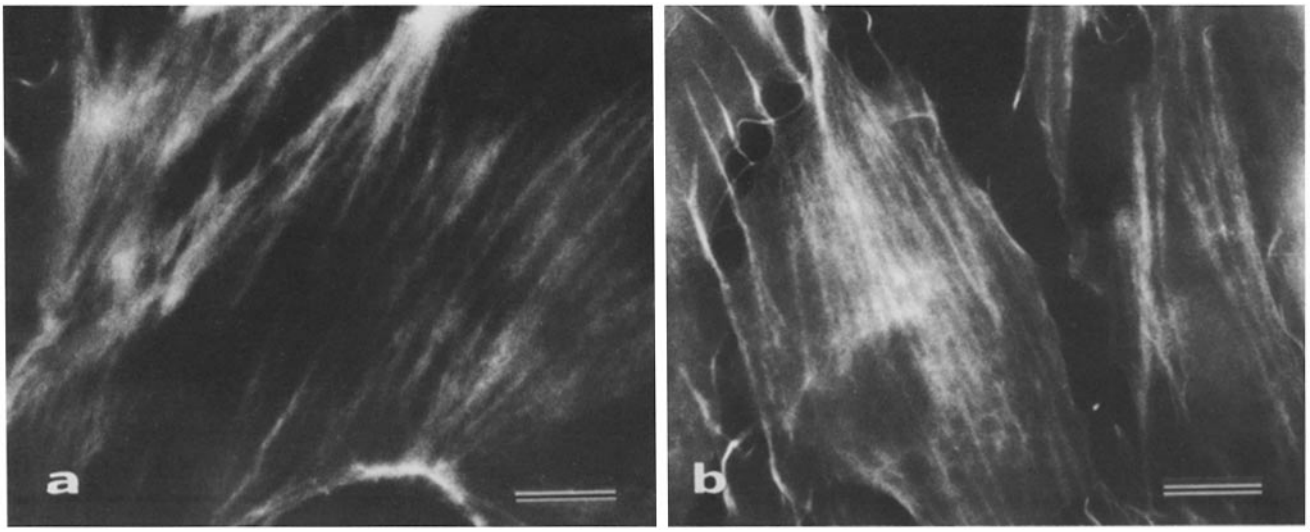

FIGURE 5 (a) Detergent-treated PtK_2 cell exposed to actin-LR in the presence of 2 mM ATP. ATP does not prevent actin-LR from binding to stress fibers; (b) glycerinated PtK_2 cell exposed first to unlabeled actin and then to actin-LR. Actin-LR was not inhibited from binding to the stress fibers. Bars, 10 μm. × 1,500 (a); × 1,300 (b).

fluorescence was more diffusely distributed along the stress fiber and in the cell (Fig. 5*b*). If the cell models were fixed in 3% paraformaldehyde and washed with standard salt solution (38) before incubation with monomer actin-LR, there was no binding to any elements of the cytoskeleton.

Addition of Fluorescent Alpha-actinin to Cell Models

Alpha-actinin-LR addition to cell models of PtK_2 and gerbil fibroma cells invariably produced a striated pattern along stress fibers and also stained cell junctions, attachment plaques, and ruffles (Fig. 6, *a–d*). In addition, the foci of dome-like structures in gerbil fibroma cells were also stained. The periodicity of alpha-actinin-LR along stress fibers was longer in gerbil fibroma cells than it was in PtK_2 cells (Fig. 6*c* vs. 6*a*). When the same alpha-actinin-LR was microinjected into living nonmuscle cells, similarly striated stress fibers were also observed (Fig. 6*e*). If cell models were pretreated with unlabeled alpha-actinin and then stained with alpha-actinin-LR, the binding appeared just as it did with alpha-actinin-LR alone. No binding was found if cell models were fixed with paraformaldehyde before addition of alpha-actinin-LR. Cells that had been grown in medium containing 20 mM azide and 10 mM 2-deoxyglucose for 1.5 h to cause stress fiber breakdown (39), and then permeabilized and exposed to alpha-actinin-LR, were filled with fluorescent aggregates (Fig. 5*f*) that were identical to treated cells stained with alpha-actinin antibody (39). When alpha-actinin-LR was added to cytoskeletons of chick fibroblasts (Fig. 7, *a* and *b*), stress fiber staining was continuous rather than banded. The leading edge of these fibroblasts also bound alpha-actinin-LR strongly as did an arc of material located between the leading edge of the cell and the nucleus. Similar arcs in other fibroblast cytoskeletons bound actin-LR (Fig. 3*b*).

PtK_2 cells permeabilized during mitosis also bound alpha-actinin-LR (Fig. 8, *a–d*). In anaphase cells, the concentration of alpha-actinin-LR was greater outside the spindle area than between the separated chromosomes (Fig. 8*a*). In telophase, alpha-actinin-LR binding was slightly higher on either side of the spindle (Fig. 8*b*), and at the beginning of cleavage, was greater in the furrow region (Fig. 8, *c* and *d*).

Addition of Fluorescent Tropomyosin to Cell Models

Tropomyosin-LR reacted at very low levels with the interphase cytoskeletons of permeabilized chick fibroblasts and epithelial cells as well as gerbil and PtK_2 cells (Fig. 9*a*). If cell models were treated first with unlabeled tropomyosin and then exposed to tropomyosin-LR, no staining at all was detected in the cells. If the permeabilized cell models were exposed first to unlabeled actin and then to tropomyosin-LR, stress fiber fluorescence was bright and continuous along the length of the fibers (Fig. 9*b*). In contrast to the extremely weak binding of tropomyosin-LR in interphase cells, a concentration of tropomyosin-LR was apparent in cleaving cells (Fig. 9, *c* and *d*). In cells midway through cleavage there was a diffuse distribution of tropomyosin-LR binding in the furrow region (Fig. 9*c*), and a marked concentration along the membrane adjacent to the furrow at the end of cytokinesis (Fig. 9*d*). When tropomyosin-LR was microinjected into living nonmuscle cells, the fluorescence along some stress fibers was continuous and along others in the same cell it was banded (Fig. 10). It generally took 4 h or longer for periodic stress fibers to stand out from the diffuse fluorescence in the cytoplasm. This is in contrast to the incorporation of actin-LR and alpha-actinin-LR, each of which was incorporated into stress fibers within 30 m after microinjection.

Addition of Fluorescent Ovalbumin and BSA to Cell Models

Neither ovalbumin-LR (Fig. 11) nor BSA-LR bound to any element of the cytoskeleton. Staining was usually observed in nuclei, vesicles, and in the perinuclear region. Microinjection of either ovalbumin-LR (47) or BSA-LR into nonmuscle cells did not lead to any staining of the cytoskeleton. Microinjected BSA-LR and ovalbumin-LR were concentrated in the perinuclear regions as well as in ruffles. Ovalbumin-LR, in addition, was concentrated in the nuclei of injected cells.

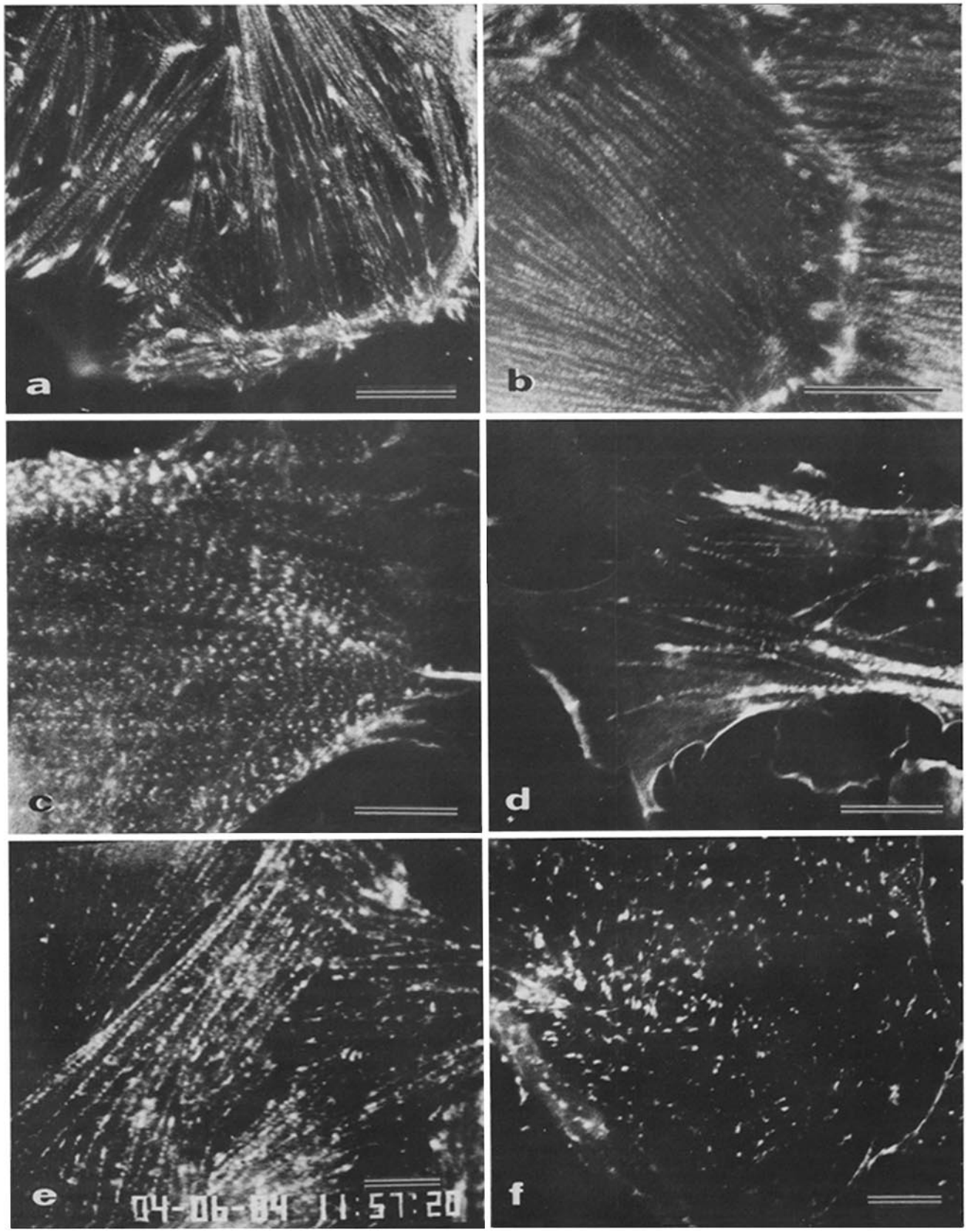

FIGURE 6 Alpha-actinin-LR binding. (*a*) In a glycerinated PtK_2 cell, fluorescence is concentrated in attachment plaques as well as in closely spaced bands along the stress fibers. (*b*) Alpha-actinin-LR binds strongly to junctions between cells as well as to stress fibers in detergent-treated PtK_2 cells. (*c*) In glycerinated gerbil fibroma cells, alpha-actinin-LR binds to stress fibers in widely spaced bands along their lengths. (*d*) Gerbil fibroma cell briefly premeabilized with cold acetone binds alpha-actinin-LR in ruffles, attachment plaques and stress fibers. (*e*) Alpha-actinin-LR microinjected into this living PtK_2 cell one day earlier binds in a striated pattern to stress fibers and also to attachment plaques. (*f*) PtK_2 exposed to NaN_3 and 2-deoxyglucose for 90 min before permeabilization for 10 s in cold acetone. Alpha-actinin-LR binds to scattered aggregates throughout the cytoplasm, the same distribution that is seen in similar cells stained with alpha-actinin antibodies. Bars, 10 μm. × 1,900 (*a*, *c*, and *d*); × 2,500 (*b*); × 1,700 (*e* and *f*).

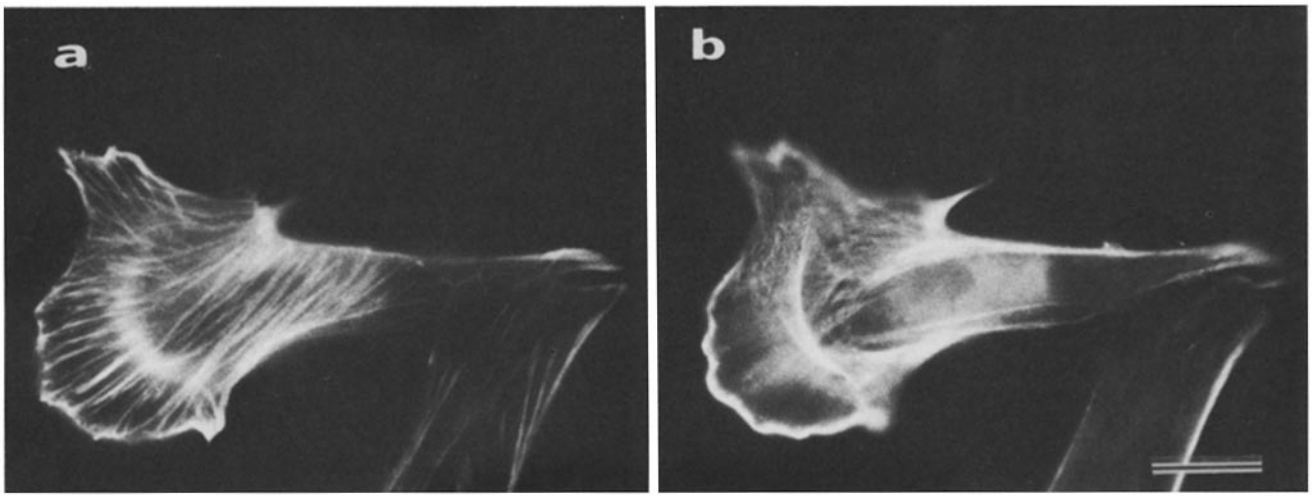

FIGURE 7 Two different focal views of the same glycerinated cardiac fibroblast illustrating the binding of alpha-actinin-LR to the stress fibers, leading edge of the cell, as well as an arc on the dorsal surface of the cell distal to the ruffle. Bar, 10 μm. × 1,400.

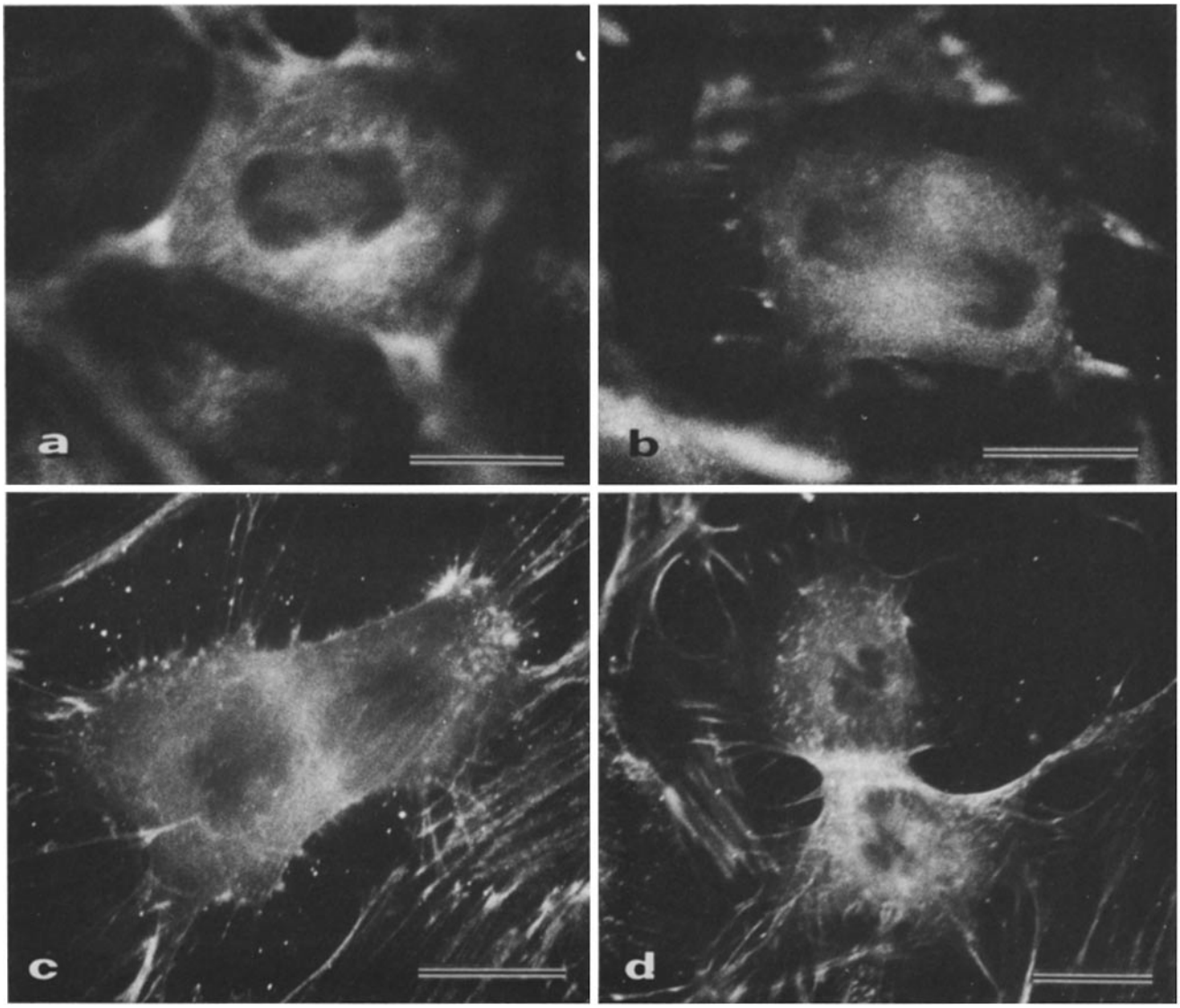

FIGURE 8 Acetone-permeabilized mitotic PtK_2 cells exposed to alpha-actinin-LR. (*a*) In mid-anaphase, no concentration of alpha-actinin-LR is observed between the separating sets of chromosomes. (*b*) At the end of anaphase a light band of alpha-actinin-LR is observed at the equator of the cell. (*c*) In early cleavage a continuous ring of alpha-actinin-LR binding is found in the cleavage furrow. (*d*) In mid cleavage a bright-band of alpha-actinin-LR is concentrated in the furrow. Bars, 10 μm. × 2,300 (*a–c*); × 1,800 (*d*).

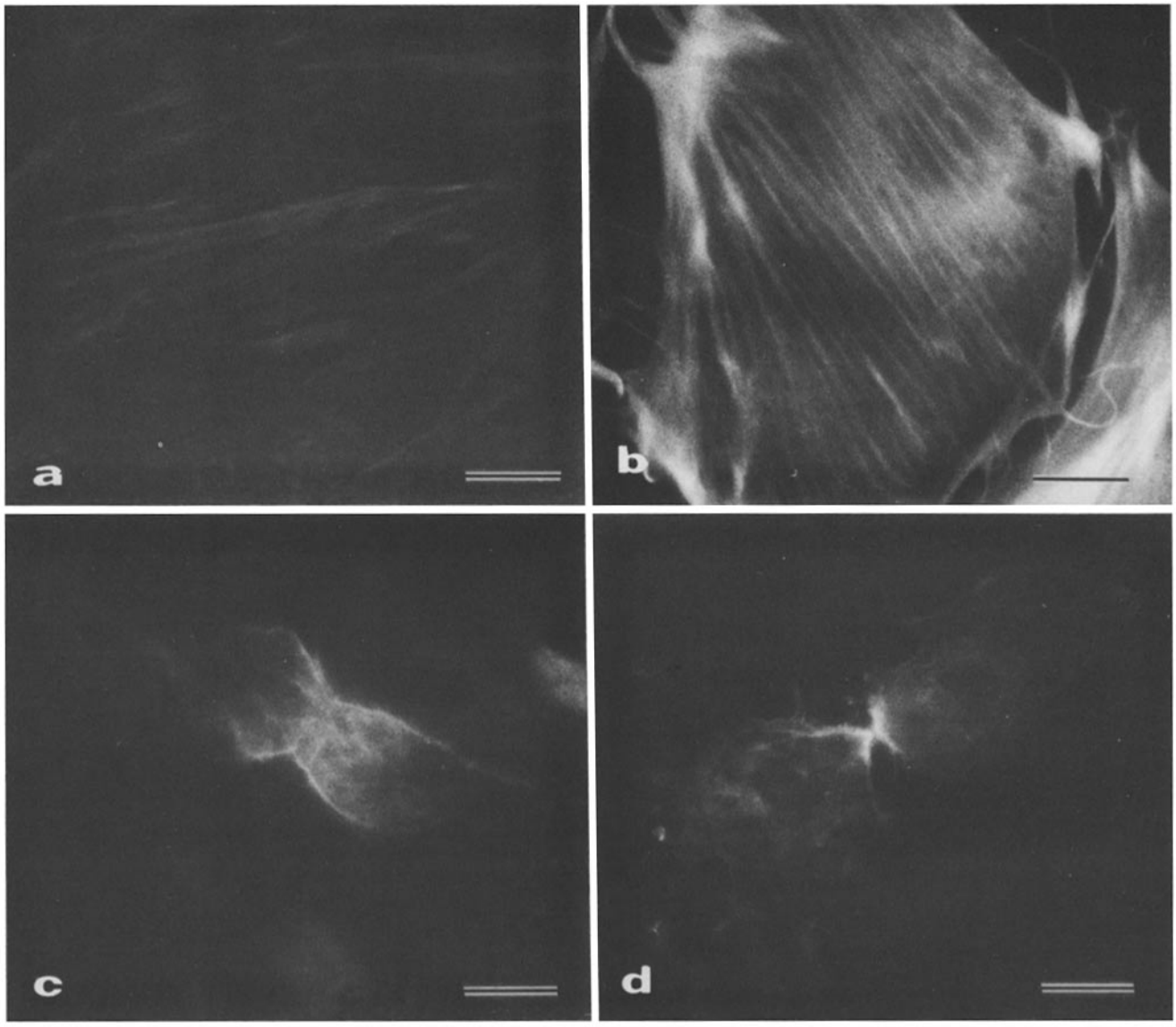

FIGURE 9 Tropomyosin-LR binding to glycerinated PtK_2 cells. (*a*) Very little tropomyosin-LR binds to the cytoskeleton in interphase cells. (*b*) This PtK_2 cell model was exposed to unlabeled actin, washed with low salt solution, and then exposed to tropomyosin-LR. Tropomyosin-LR binds to the stress fibers and periphery of the treated cell. (*c*) A diffuse distribution of fluorescence is concentrated in the furrow region of a cell glycerinated during cleavage. (*d*) At the end of cleavage, tropomyosin-LR binds along the membrane of the former cleavage furrow. Bar, 10 μm. × 1,400.

DISCUSSION

When microinjected into nonmuscle cells, fluorescently labeled actin, tropomyosin, and alpha-actinin associate with specific subcellular regions (7, 18, 35, 40, 47, 50) in patterns that closely resemble those found with antibody localization techniques in fixed cells (20–22). Our results show that labeled actin and alpha-actinin, but not tropomyosin, reacted with permeabilized cell models of PtK_2 and gerbil fibroma cells in the same way as proteins injected into living cells. Although addition of labeled actin usually produced solidly labeled stress fibers (Fig. 3, *a–c*), examples could be found of cells with striated stress fiber labeling (Fig. 3, *d* and *e*). In these cells, the pattern of banding along the fibers differed in the two cell types with the fluorescent bands closer together in the PtK_2 fibers than in the gerbil fibers, similar to the banding observed with alpha-actinin-LR staining (compare Fig. 3, *d* and *e* with Fig. 6, *a* and *c*).

Actin-LR interaction with stress fibers in the cell models could occur as a result of polymerization onto the ends of stress fiber microfilaments, binding to stress fiber myosin, or interaction with actin-binding proteins in stress fibers (e.g., alpha-actinin, filamin, etc.) In glycerinated myofibrils in the absence of ATP, actin-LR does bind to myosin where free cross-bridges are available in the H-band (Fig. 2, *c* and *d*) (34). In the presence of ATP, actin-LR does not bind to myofibrils (34). It is unlikely that in nonmuscle cells enough myosin binding sites would be free to interact with the exogenous actin in view of the high ratio of actin to myosin present in these cells (24) and the absence of H-bands in stress fibers (38). The inability of ATP (Fig. 5 *a*) or sodium pyrophosphate to block the binding of actin-LR to stress fibers also indicates that the binding site is not myosin. Our results cannot distinguish between the possibilities that actin-LR polymerized from the ends of stress fiber microfilaments or that it formed filaments that bound to the stress fibers via actin-binding

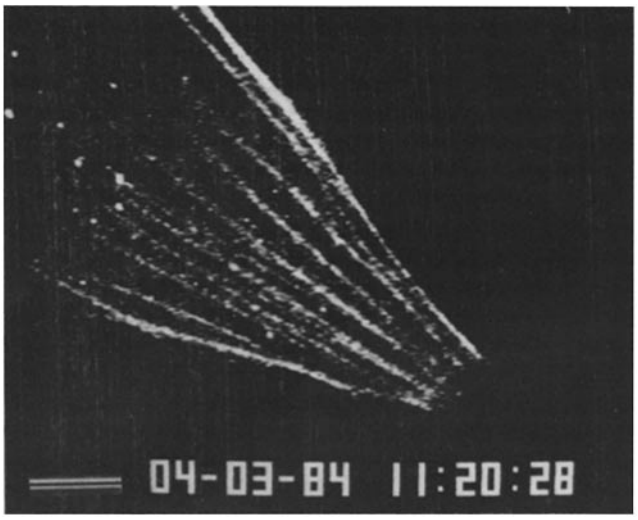

FIGURE 10 Videomicrograph of living PtK_2 cell that had been microinjected one day earlier with tropomyosin-LR. Many of the stress fibers appear striated. Bar, 10 μm. × 1,300.

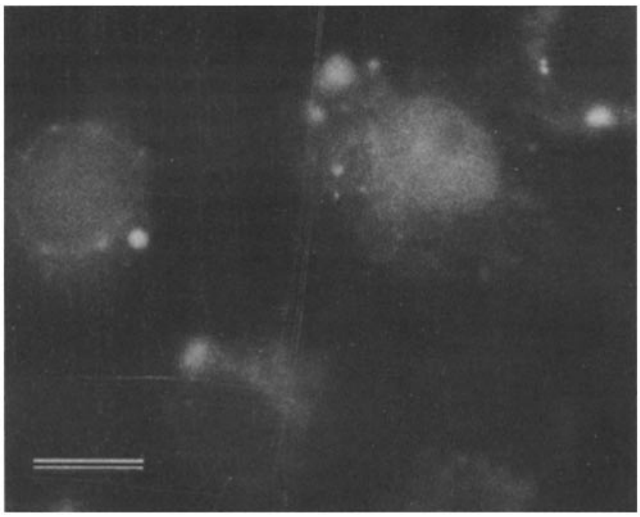

FIGURE 11 Detergent-treated PtK_2 cells exposed to ovalbumin-LR. Binding occurs in many of the nuclei and perinuclear granules but not to any elements of the cytoskeleton. Bar 10 μm. × 1,500.

proteins like alpha-actinin in the dense bodies and attachment plaques. For actin-LR to polymerize from the ends of microfilaments, capping proteins (9) would have to be lacking. This would be in direct contrast to the capped actin filaments in myofibrils (34).

When cell models were exposed to unlabeled actin followed by actin-LR, fluorescence remained localized along the length of the stress fibers (Fig. 5*b*), although the amount of background fluorescence was higher than when actin-LR alone was added (compare Fig. 5*b* with Fig. 3*c*). Myosin and other actin-binding proteins should have been fully complexed by the unlabeled actin in this experiment. Therefore, the staining observed in these pretreated cells may have resulted from elongation of existing stress fiber microfilaments or from polymerization of actin-LR onto the bound, unlabeled exogenous actin. We never observed periodic actin-LR patterns in these blocking experiments indicating that the periodic patterns represent short filaments that can grow further.

It is unlikely that the actin binding we observed was passive sticking of actin-LR to stress fibers or other elements of the cytoskeleton because when the cells were fixed prior to actin-LR addition no binding occurred. Furthermore, neither ovalbumin-LR nor BSA-LR bound to unfixed cytoskeletons indicating that the LR dye itself is not responsible for any binding to elements of the cytoskeleton. It is clear also that there was no binding of actin-LR to the extensive, wavy networks of keratin and vimentin found in PtK_2 cells (9, 33). As a control for actin microinjection experiments, Glacy (13) fixed and permeabilized chick fibroblasts and myocytes, added labeled actin, and found no fluorescence associated with stress fibers or myofibrils. This was interpreted as evidence that a living cell is necessary for actin incorporation. Our results demonstrated that fixation of permeabilized cells abolishes actin-LR binding in cell models and that a living cell is not required for incorporation of actin into the cytoskeleton. Our patterns of actin-LR binding in cell models mirror actin incorporation in microinjected cells by others (13, 17) and ourselves (40, this paper) and actin localization in cells that have been stained with actin antibodies or actin-binding probes (22, 29). This is not to say that actin-LR addition in cell models occurs in the same way as the incorporation of microinjected actin into living cells. We can only say from these experiments that it occurs in the same locations in nonmuscle cells.

The localization of alpha-actinin-LR that we have found in chick, PtK_2, and in gerbil fibroma cells confirms the results reported by Geiger (12) on the incorporation of this protein into models of chicken gizzard fibroblasts and Madin Darby canine kidney cells. In those cells, Geiger showed that all areas that were known from antibody studies to contain alpha-actinin would combine with alpha-actinin-LR in cell models. Our results further show that the spacing between the bands of alpha-actinin fluorescence in gerbil fibroma cell models was longer than in the epithelial PtK_2 cell models. This is the same relationship that is found when the two different cell types are stained with alpha-actinin antibodies (38) and is consistent with the models of the stress fiber structure Sanger et al. recently proposed (38). Our attempts to block the binding of alpha-actinin-LR to cell models by first exposing the cells to unlabeled alpha-actinin were unsuccessful, suggesting that alpha-actinin binds to itself. This interpretation is supported by our work on the binding of alpha-actinin to the Z-bands of muscle which also indicates that alpha-actinin binds to itself (34). Masaki and Takaita (23) demonstrated that alpha-actinin self-associated in 0.1 M KCl, but was prevented from self-association in 1 mM bicarbonate solution. We have found that alpha-actinin-LR did not associate with the Z-bands of myofibrils in the presence of 1 mM sodium bicarbonate but did bind when the myofibrils were stained in the presence of 0.1 M KCl (34). Furthermore, the binding was not prevented by prior exposure of the myofibrils to unlabeled alpha-actinin.

In contrast to these cell types, glycerinated chick cardiac fibroblasts bound alpha-actinin-LR in a continuous pattern along the stress fibers (Fig. 7, *a* and *b*). Alpha-actinin antibody staining of these fibroblasts often shows alpha-actinin to be distributed continuously along the complete length of the stress fibers (data not shown). Another area in chick fibroblasts that reacted with alpha-actinin-LR was an arc positioned between the nucleus and leading edge of the cell (Fig. 7, *a* and *b*). Similar arcs were seen frequently in other fibroblast

models where they bound actin-LR (Fig. 3*b*) but not tropomyosin-LR. Soranno and Bell (42) reported that birefringent arcs that stained with actin antibody formed near the leading edge of locomoting human lung fibroblasts. They speculated that the arcs resulted from condensations of microfilaments. In our fibroblast models, the arcs bound alpha-actinin-LR and actin-LR in the same way as the ruffles, thus lending support to this idea.

In contrast to actin-LR and alpha-actinin-LR, tropomyosin-LR did not react with permeabilized cell models of chick cells, PtK_2, and gerbil fibroma cells in patterns mimicing antibody localization studies (38). Tropomyosin-LR bound very faintly to stress fibers in chick, gerbil, and PtK_2 cell models (Fig. 9*a*) but this weak binding could be increased if the cell models were pretreated with unlabeled actin before exposure to tropomyosin-LR (Fig. 9*b*). In glycerinated myofibrils, tropomyosin-LR binds to the thin filaments only if the native tropomyosin is removed first (34). This suggests that most of the stress fiber actin in the cell model is fully complexed with tropomyosin and other actin-binding proteins, and only if exogenous actin is allowed to polymerize along the stress fiber, will tropomyosin-LR bind to the fibers. The very low level of continuous tropomyosin-LR binding along stress fibers in cytoskeletons may be due to a small population of actin filaments lacking tropomyosin or to stress fiber microfilaments incompletely complexed with tropomyosin and actin-binding proteins such as alpha-actinin. It is also possible that when cells are premeabilized, actin filaments lacking tropomyosin may be extracted. In both glycerinated muscle (34) and nonmuscle cells (Fig. 9*a*), tropomyosin-LR does not react with areas where alpha-actinin is concentrated, i.e., Z-bands, cell junctions, attachment plaques, and ruffles. Antibody studies (12, 20, 38) show such areas also lack tropomyosin.

Tropomyosin-LR did bind to cleavage furrows in cell models (Fig. 9, *c* and *d*) as did actin-LR (Fig. 4, *b* and *c*) and alpha-actinin-LR (Fig. 8, *b–d*). This is the only place where both tropomyosin-LR and alpha-actinin-LR bound the same area of the cell. Since both proteins will bind to actin that is free of tropomyosin (34), it may be that microfilaments lacking tropomyosin are present in the furrows. Such microfilaments would be more labile than those complexed with tropomyosin (24) and might be intermediates in a structure that must assemble and disassemble in a short period of time (28, 36).

Although actin-LR and alpha-actinin-LR do not need a living cell to become associated with their endogenous counterparts, tropomyosin-LR does require a living cell before it can be incorporated into stress fibers. The staining patterns produced in our cell models resemble closely those in cells microinjected with alpha-actinin (7, Fig. 6*e*), or actin (16, 17, 40; Fig. 3*f*), but not tropomyosin (50, Fig. 10). The incorporation of microinjected fluorescent tropomyosin into stress fibers of living cells (50, Fig. 10) may be due to an exchange of native and fluorescently labeled tropomyosin in living cells that we do not see in cell models. We also did not see this exchange in myofibrils (34). Alternatively, microinjected tropomyosin may induce the polymerization of nonfilamentous actin into the stress fiber.

Fluorescent analog cytochemistry (44–46) has the potential for making dynamic processes in cells visible with the light microscope. A major concern in these studies is that the functional properties of the labeled molecule be retained. Our studies show that myofibrils and cell models provide excellent assay systems for testing the specificity of labeled contractile proteins that are to be microinjected into living cells. This approach also indicates the extent to which various proteins can self-associate or react with other proteins in the absence of metabolic controls that a living cell would normally impose.

The authors thank Mark B. Pochapin for his help in microinjecting actin into cells. We are also indebted to David J. Casso and John M. Sanger for their capable photographic assistance during the course of this work.

This research was supported by grants from the National Institutes of Health (HL-15835 to the Pennsylvania Muscle Institute and GM-25653 to J. W. Sanger and J. M. Sanger).

Received for publication 26 January 1984, and in revised form 18 May 1984.

REFERENCES

1. Aubin, J. E., K. Weber, and M. Osborn. 1979. Analysis of actin and microfilament-associated proteins in the mitotic spindle and cleavage furrow of PtK_2 cells by immunofluorescence microscopy. *Exp. Cell Res.* 124:93–109.
2. Barak, L. S., E. A. Nothnagel, E. F. DeMarco, and W. W. Webb. 1981. Differential staining of actin in metaphase spindles with 7-nitrobenz-2-oxa-1,3 diazole phallacidin and fluorescent DNase: is actin involved in chromosomal movement? *Proc. Natl. Acad. Sci. USA.* 78:3034–3038.
3. Barak, L. S., R. R. Yocum, E. A. Nothnagel, and W. W. Webb. 1980. Fluorescence staining of the actin cytoskeleton in living cells with 7-nitrobenz-2-oxa-1,3-dazole phallacidin. *Proc. Natl. Acad. Sci. USA.* 77:980–984.
4. Blikstad, I., S. Eriksson, and L. Carlsson. 1980. Alpha-actin promotes polymerization of actin from profilactin. *Eur. J. Biochem.* 109:317–323.
5. Brandtzaeg, P. 1973. Conjugates of immunoglobulin G with different fluorochromes. I. Characterization by anionic-exchange chromatography. *Scand. J. Immunol.* 2:273–290.
6. Cande, W. Z., E. Lazarides, and J. R. McIntosh. 1977. A comparison of the mammalian mitotic spindle as seen by indirect immunofluorescence. *J. Cell Biol.* 72:552–567.
7. Feramisco, J. R. 1980. Microinjection of fluorescently labeled alpha-actinin into living fibroblasts. *Proc. Natl. Acad. Sci. USA.* 76:3967–3971.
8. Feramisco, J. R., and K. Burridge. 1980. A rapid purification of alpha-actinin, filamin, and a 130,000 dalton protein from smooth muscle. *J. Biol. Chem.* 255:1194–1199.
9. Franke, W. W., C. Grund, M. Osborn, and K. Weber. 1978. The intermediate-sized filaments in rat kangaroo PtK_2 cells. I. Morphology *in situ*. *Eur. J. Cell Biol.* 17:365–391.
10. Fuchtbauer, A., B. M. Jockusch, H. Maruta, M. W. Kilimann, and G. Isenberg. 1983. Disruption of microfilament organization after injection of F-actin capping proteins into living tissue culture cells. *Nature (Lond.).* 304:361–364.
11. Fugiwara, K., M. E. Porter, and T. D. Pollard. 1978. Alpha-actinin localization in the cleavage furrow during cytokinesis. *J. Cell Biol.* 79:268–275.
12. Geiger, B. 1981. The association of rhodamine-labelled alpha-actinin with actin bundles in demembranated cells. *Cell Biology International Reports.* 5:627–634.
13. Glacy, S. D. 1982. Subcellular distribution of rhodamine-actin microinjected into living fibroblastic cells. *J. Cell Biol.* 97:1207–1213.
14. Gordon, S. R. 1983. The localization of actin in dividing corneal endothelial cells demonstrated with nitrobenzoxadiazole phallacidin. *Cell Tissue Res.* 229:533–539.
15. Gordon, W. E. 1978. Immunofluorescent and ultrastructural studies of "sarcomeric" units in stress fibers of cultured non-muscle cells. *Exp. Cell Res.* 117:253–260.
16. Herman, I. M., and T. D. Pollard. 1979. Comparison of purified anti-actin and fluorescent-heavy meromyosin staining patterns in dividing cells. *J. Cell Biol.* 80:509–520.
17. Kreis, T. E., B. Geiger, and J. Schlessinger. 1982. Mobility of microinjected rhodamine actin within living chicken gizzard cells determined by fluorescence photobleaching recovery. *Cell.* 29:835–845.
18. Kreis, T., K. H. Winterhalter, and W. Birchmeier. 1979. *In vivo* distribution and turnover of fluorescently labeled actin microinjected into human fibroblast. *Proc. Natl. Acad. Sci. USA.* 76: 3814–3818.
19. Laemmli, U. K. 1970. Cleavage of structural proteins during the assembly of the head of bacteriophage T_4. *Nature (Lond.).* 227:680–685.
20. Lazarides, E. 1975. Tropomyosin antibody: the specific localization of tropomyosin in non-muscle cells. *J. Cell Biol.* 65:549–561.
21. Lazarides, E., and K. Burridge. 1975. Alpha-actinin immunofluorescent localization of a muscle structural protein in non-muscle cells. *Cell.* 6:289–298.
22. Lazarides, E., and K. Weber. 1974. Actin antibody: the specific visualization of actin filaments in non-muscle cells. *Proc. Natl. Acad. Sci. USA.* 71:2268–2272.
23. Masaki, T., and O. Takaita. 1969. Some properties of chicken alpha-actinin. *J. Biochem. (Tokyo).* 66:637–643.
24. Maupin-Szamier, P., and T. D. Pollard. 1978. Actin filament destruction by osmium tetroxide. *J. Cell Biol.* 77:837–852.
25. Pardee, J. D., and J. A. Spudich. 1982. Purification of muscle actin. *Methods Enzymol.* 85:271–289.
26. Pochapin, M. B., J. M. Sanger, and J. W. Sanger. 1983. Microinjection of lucifer yellow CH into sea urchin eggs and embryos. *Cell Tissue Res.* 234:309–318.
27. Pollard, T. E., and R. Weihing. 1974. Actin and myosin and cell movement. *CRC Crit. Rev. Biochem.* 2:1–65.
28. Sanger, J. M., and J. W. Sanger. 1980. Banding and polarity of actin filaments in interphase and cleaving cells. *J. Cell Biol.* 86:568–575.
29. Sanger, J. W. 1975. Changing patterns of actin localization during cell division. *Proc. Natl. Acad. Sci. USA.* 72:1913–1916.
30. Sanger, J. W. 1975. The presence of actin during chromosomal movement. *Proc. Natl. Acad. Sci. USA.* 72:2451–2455.

31. Sanger, J. W. 1975. Intracellular localization of actin with fluorescently labelled heavy meromyosin. *Cell Tissue Res.* 161:432–444.
32. Sanger, J. W. 1977. Mitosis in beating cardiac myoblasts treated with cytochalasin-B. *J. Exp. Zool.* 201:463–469.
33. Sanger, J. W. 1977. Nontubulin molecules in the spindle. Mitosis: facts and questions. M. Little, N. Paweletz, C. Petzelt, H. Ponstingl, D. Schroeter, and H.-P. Zimmermann, editors. Springer-Verlag, Heidelberg. 98–113.
34. Sanger, J. W., B. Mittal, and J. M. Sanger. 1984. Analysis of myofibrillar structure and assembly using fluorescently labeled contractile proteins. *J. Cell Biol.* 98:825–833.
35. Sanger, J. W., M. B. Pochapin, B. Mittal, and J. M. Sanger. 1983. Dynamics of alpha-actinin distribution in living non-muscle and muscle cells. *J. Cell Biol.* 97:280*a*. (Abstr.)
36. Sanger, J. W., and J. M. Sanger. 1979. The cytoskeleton and cell division. *Methods Achiev. Exp. Pathol.* 8:110–142.
37. Sanger, J. W., J. M. Sanger, and J. Gwinn. 1979. Actin and the mitotic spindle. *In* Motility in Cell Function, F. A. Pepe, J. W. Sanger, and V. T. Nachmias, editors. Academic Press, Inc., New York. 313–323.
38. Sanger, J. W., J. M. Sanger, and B. M. Jockusch. 1983. Differences in the stress fibers between fibroblasts and epithelial cells. *J. Cell Biol.* 96:961–969.
39. Sanger, J. W., J. M. Sanger, and B. M. Jockusch. 1983. Differential response of three types of actin filament bundles to depletion of cellular ATP levels. *Eur. J. Cell Biol.* 31:197–204.
40. Sanger, J. W., J. M. Sanger, T. E. Kreis, and B. M. Jockusch. 1980. Reversible translocation of cytoplasmic actin into the nucleus caused by dimethyl sulfoxide. *Proc. Natl. Acad. Sci. USA.* 77:5268–5272.
41. Smillie, L. B. 1982. Preparation and identification of alpha- and beta-tropomyosins. *Methods Enzymol.* 85:234–241.
42. Soranno, T., and E. Bell. 1982. Cytostructural dynamics of spreading and translocating cells. *J. Cell Biol.* 95:127–136.
43. Suzuki, A., D. E. Goll, I. Singh, R. E. Allen, R. M. Robson, and M. H. Stromer. 1976. Some properties of purified skeletal muscle alpha-actinin. *J. Biol. Chem.* 251:6860–6870.
44. Taylor, D. L., P. A. Amato, K. Luby-Phelps, and P. McNeil. 1984. Fluorescent analog cytochemistry. *Trends Biochem. Sci.* 9:88–91.
45. Wang, Y. L., J. M. Heiple, and D. L. Taylor. 1982. Fluorescent analog cytochemistry of contractile proteins. *Methods Cell Biol.* 25B:1–11.
46. Wang, K., J. R. Feramisco, and J. F. Ash. 1982. Fluorescent localization of contractile proteins in tissue culture cells. *Methods Enzymol.* 85:514–562.
47. Wang, Y. L., and D. L. Taylor. 1979. Distribution of fluorescently labeled actin in living sea urchin eggs during early development. *J. Cell Biol.* 82:672–679.
48. Wang, Y. L., and D. L. Taylor. 1980. Preparation and characterization of a new molecular cytochemical probe: 5-iodoacetamide fluorescein-labeled actin. *J. Histochem. Cytochem.* 28:1198–1206.
49. Weber, K., and U. Groeschel-Stewart. 1974. Antibody to myosin: the specific visualization of myosin containing filaments in non-muscle cells. *Proc. Natl. Acad. Sci. USA.* 71:4561–4564.
50. Wehland, J., and K. Weber. 1980. Distribution of fluorescently labeled actin and tropomyosin after microinjection in living tissue culture cells observed with TV image intensification. *Exp. Cell Res.* 127:397–408.
51. Woods, E. F. 1967. Molecular weight and subunit structure of tropomyosin B. *J. Biol. Chem.* 242:2859–2871.
52. Zigmond, S. H., J. J. Otto, and J. Bryan. 1979. Organization of myosin in a submembraneous sheath in well-spread human fibroblasts. *Exp. Cell Res.* 119:205–219.